

Photoactive Blends of Poly(*para*-phenylenevinylene) (PPV) with Methanofullerenes from a Novel Precursor: Photophysics and Device Performance

C. J. Brabec*,† A. Cravino,† G. Zerza,† and N. S. Sariciftci†

Christian Doppler Laboratory for Plastic Solar Cells, Johannes Kepler University, A-4040 Linz, Austria

R. Kiebooms‡ and D. Vanderzande§

Institute for Materials Research, Material Physics Division, Wetenschapspark 1, B-3590 Diepenbeek, Belgium
Institute for Materials Research, Chemistry Division, University Campus Gebouw D.
B-3590 Diepenbeek, Belgium

J. C. Hummelen||

Stratingh Institute and Materials Science Center, University of Groningen, Nijenborgh 4,
9747 AG Groningen, The Netherlands

Received: September 20, 2000

Homogeneous blends of a processable methanofullerene, [6,6]-phenyl C₆₁-butyric acid methyl ester (PCBM), with poly(*para*-phenylenevinylene) (PPV) synthesized using a novel nonionic precursor route were produced. These photoactive blends have been investigated by excited-state spectroscopy and by photocurrent measurements. UV–vis and IR absorption measurements, as well as luminescence spectroscopy, were used to monitor the conversion process of the precursor polymer to the PPV in blends with PCBM. The presence of PCBM did not influence the successful conversion process. The occurrence of photoinduced charge transfer, well-known for blends of substituted PPV with fullerenes, was evidenced in composites of PPV/PCBM by the strong quenching of the PPV luminescence. LESR (light induced electron spin resonance) and PIA (photoinduced absorption) studies confirmed the occurrence of photoinduced electron transfer from the PPV to PCBM within the bulk of solid state composite films. Photovoltaic devices made from PPV/PCBM blends showed power efficiencies of up to 0.25% under intense white light illumination. The spectral-photocurrent excitation profile was observed to follow closely the absorption spectrum of the PPV.

Introduction

It is indeed intriguing and very attractive to think of large area photovoltaic elements based on thin plastic films with very low cost cut from rolls and deployed on permanent structures and surfaces. To fulfill these low cost and large area requirements, cheap production technologies for large scale coating must be applied to a low cost material class. Polymeric photovoltaic cells have the potential of such low cost photocells. The flexibility of chemical tailoring of desired properties, as well as the cheap technology already well-developed for all kinds of plastic thin film applications, meet exactly the above formulated demands for cheap photovoltaic device production. The mechanical flexibility of plastic materials is welcome for all photovoltaic applications onto curved surfaces in indoor as well as outdoor applications.

The efficiencies of the first polymeric solar cells, based on hole conducting conjugated polymers (mainly polyacetylene),

were rather discouraging.¹ Encouraging breakthrough to higher efficiencies was achieved by switching to different classes of electron donor type conjugated polymer (polythiophene (PT), poly(*p*-phenylenevinylene) (PPV) and their derivatives) and by mixing them with suitable electron acceptors.^{2,3} Prototypes of photovoltaic devices based on a polymeric donor/acceptor network showed solar energy conversion efficiencies of around 1%.⁴ The photovoltaic properties and the photophysics of conjugated polymer/fullerene solid composites have been especially well investigated in the last years.⁵

Initial efforts on photovoltaic devices using conjugated polymers were with polyacetylene¹ and some polythiophenes.^{6,7} From the conjugated polymers of the first generation, PPV was the most successful candidate for single layer polymer photovoltaic devices.⁸ Unsubstituted PPV is generally produced from a soluble precursor polymer with subsequent thermal conversion. The radiative recombination channels of the injected electrons and holes within PPV, and its derivatives, which resulted in light emitting diodes (LED^{9–12}), opened this class of materials for high electroluminescence quantum efficiency optoelectronic devices. Furthermore, it was found, that the same LED devices, under reverse bias, exhibit excellent sensitivity as photodiodes.¹³ In forward bias, tunneling injection diodes exhibit relatively high efficiency electroluminescence, which is promising for flat panel and/or flexible, large area display applications. In reverse bias, on the other hand, the devices exhibit a strong photoresponse

* To whom correspondence should be addressed. Christoph Josef Brabec, Christian Doppler Laboratory for Plastic Solar Cells, Institute of Chemistry/Physical Chemistry, Johannes Kepler University Linz, Austria. Tel.: +43 732 2468 8766. Fax: +43 732 2468 8770. E-mail: christoph.brabec@jk.uni-linz.ac.at.

† Christian Doppler Laboratory for Plastic Solar Cells, Johannes Kepler University.

‡ Institute for Materials Research, Material Physics Division, Wetenschapspark.

§ Institute for Materials Research, Chemistry Division, University Campus Gebouw D. B-3590 Diepenbeek.

|| Stratingh Institute and Materials Science Center, University of Groningen.

with a quantum yield $>20\%$ (el/ph at -10 V reverse bias).¹³ Compared to the new generation of substituted PPVs, the PPV from the precursor polymer is still interesting due to its environmental as well as mechanical stability.

Independently, Santa Barbara group and Osaka group reported studies on the photophysics of mixtures and bilayers of conjugated polymers with fullerene^{2,5,14–22}. The experiments clearly evidenced an ultrafast (subpicosecond), reversible, metastable photoinduced electron transfer from conjugated polymers onto the C_{60} in solid films. Once the photoexcited electron is transferred to an acceptor unit, the resulting radical cation (positive polaron) species on the conjugated polymer backbone is known to be highly delocalized and stable as shown in electrochemical and/or chemical oxidative reaction (p-doping) studies. The long lifetime of the charge transferred state and the high quantum efficiency of this process ($\sim 100\%$) especially favored the development of photocells using such blends.

Because of the water solubility of the precursor PPV, fullerene acceptors could not be mixed into unsubstituted PPV up to now. Recently, it was reported that methanol soluble fullerenes allow to cast PPV/fullerene composites from solution.²³ A complete different approach to overcome this solubility problem is the development of a new class of PPV precursor polymers that are soluble in common organic solvents.²⁴

In this paper, we report on the observation of photoinduced charge transfer in composites of PPV from a novel precursor polymer with a highly soluble methanofullerene (PCBM). The performance of photovoltaic devices from this PPV/PCBM composites are discussed and compared to the performance of state of the art devices from alkoxy-PPV/PCBM blends.

Experimental Section

The synthesis is based on the precursor method first reported by Louwet et al.^{24b} This precursor method makes use of the formation of a double bond through thermal elimination of a sulfoxy side chain. The main advantages of these precursor polymers are their increased stability as compared to the standard Wessling route,²⁵ solubility in organic solvents and the elimination of noncorrosive materials under thermal treatment. The modified synthesis was used to synthesize the poly(*n*-octylsulfinyl-*para*-phenylene ethylene) precursor. The typical procedure for the synthesis of the monomer and the polymer is given below. Molecular weight M_w of the precursor was determined with gel permeation chromatography (GPC) in tetrahydrofuran (THF) against a polystyrene standard. Poly(*n*-octylsulfinyl-*para*-phenylene ethylene) precursor has a molecular weight M_w of 184 000 g/mol and polydispersity (PD) of 2.48. The glass transition temperature (T_g) of the precursor polymer is 63 °C.

The chemical structure of the compounds investigated in this study are shown in Figure 1 together with the conversion process of the precursor polymer to PPV. The PPV, obtained by thermal conversion of a *n*-octylsulfinyl precursor polymer, was used as the electron donor, whereas the electron acceptor was [6,6]-Phenyl C_{61} -butyric acid methyl ester²⁶ (PCBM). The enhanced solubility of PCBM compared to C_{60} allows a high fullerene/conjugated polymer ratio and strongly supports the formation of donor/acceptor bulk heterojunctions. Samples for investigations were produced by casting from a 1% wt./vol. toluene solution either on KBr pellets (for IR investigations, but also for UV-vis absorption and luminescence measurements) or on glass substrates (for luminescence, UV-vis absorption and PIA measurements). Partial conversion of the cast films was performed at 180 °C for 4 h in a vacuum better than 10^{-2} mbar,

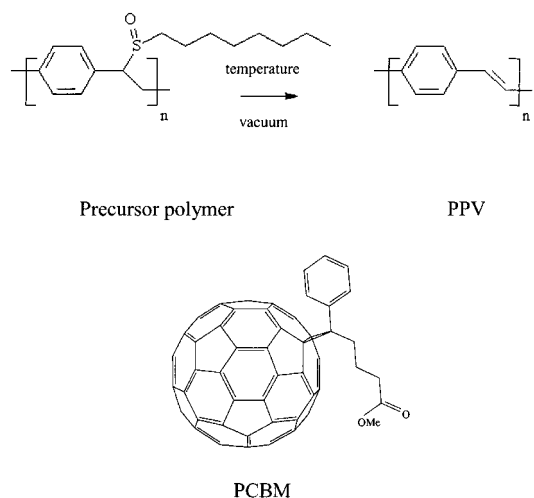


Figure 1. Chemical structure of the single compounds and the conversion scheme of the precursor polymer to PPV.

whereas full conversion was performed at a vacuum better than 10^{-4} mbar as suggested recently by²⁵ at temperatures between 100 °C and 180 °C for 8 h.

Photoinduced FTIR (PIA-FTIR) measurements were performed on composites with equal weight ratios of PPV to PCBM (1:1). Infrared Active Vibration (IRAV) spectra were recorded on a Bruker IFS 66S spectrometer with a liquid nitrogen cooled MCT detector. The vacuum during all measurements was better than 10^{-5} mbar. The photoinduced charges in the infrared absorption spectra of the conjugated polymer were observed by measuring 10 single beam spectra under illumination of the polymer sample and referencing them to 10 single beam spectra taken in the dark. The samples were illuminated through a quartz window of the cryostat by an Ar^+ laser (488 nm, 20 mW/cm²). For a better signal-to-noise ratio 200 repetitions of the measuring sequence described above were accumulated.

The room-temperature absorption and luminescence spectra were measured by a HP UV-vis spectrometer with a CCD array and by a Hitachi luminescence spectrometer with a photomultiplier as detection unit, respectively. For taking low-temperature luminescence spectra the samples were placed in an evacuated liquid nitrogen bath cryostat. The chopped 488 nm beam of an argon laser served as pump source. Luminescence was then measured with a monochromator and a Si photodiode by a lock-in amplifier. The PIA measurements were made in a two beam technique. A chopped argon-ion laser beam was used to generate photoexcited states in the sample, which were detected by analyzing the change in transmission of a white light tungsten halogen lamp. Transmission was measured using a lock-in amplifier with a monochromator and a Si detector. In all cases, samples were mounted to the coldfinger of the liquid nitrogen cryostat at a vacuum of 10^{-5} mbar.

ESR and LESR spectra were taken on free-standing films, either unconverted, partially converted or fully converted. The measurements were performed on a Bruker EMX spectrometer with a 200 MHz broadband bridge and a rectangular high Q cavity. The samples were illuminated by an Ar^+ laser (488 nm, 70 mW) through a 50% grid in the front of the cavity. Samples for LESR investigations were prepared in 3 mm Wilmad EPR tubes by insertion of the free-standing films described above. PPV-PCBM composites were prepared as free-standing films, filled in the tube in the presence of 2-methyl THF. Tubes were deoxygenated by subsequent freeze-thaw cycles and sealed. Measurements were performed at 100 K. 2-Methyl THF gives a transparent glass when freezing down to 100 K. Dark spectra

were taken for reference.²⁷ Spectra were evaluated by calculating the g -value $g = h\nu/\mu_B B$, with h as the Planck constant, ν the frequency of the X band spectrometer, μ_B the Bohr magneton, and B the applied magnetic field. No PCBM could be washed out from the free-standing PPV/PCBM film in 2-methyl THF.

ITO/glass substrates were cleaned in ultrasonic baths of acetone, methanol, and 2-propanol, followed by oxygen plasma treatment. Poly(ethylene dioxythiophene) doped with polystyrene sulfonic acid (PEDOT:PSS, Bayer AG) was spin-coated to a thickness of 100 nm on top of the ITO from an aqueous solution. The photoactive layer consisting of PPV/PCBM (1:3 wt. ratio) was spin-coated from solution (0.5% wt./vol. precursor polymer in chloroform) to a thickness of 100 – 150 nm. Conversion was performed by a thermal step of 100 °C for 8 h under 10^{-5} mbar. For the anode, a two-layer deposition of LiF/Al was performed. A small amount of LiF was first thermally deposited (10^{-6} mbar) with an average thickness of 0.6 nm onto the active layer. Finally, the aluminum cathode was thermally deposited through a shadow mask to define a device area of 5 mm². Device fabrication was performed in a drybox under an argon atmosphere. As a reference diode, poly(2-methoxy-5-(3,7-dimethyloxy)-*para*-phenylenevinylene) (MDMO-PPV):PCBM (1:4 by wt) photodiodes were produced by spin-coating on top of the PEDOT to a thickness of 100 nm from a toluene solution and supplying them with electrodes as described above.

I/V curves were recorded by a Keithley 2400 Source Meter in inert atmosphere at room temperature under illumination with 80 mW/cm² white light from a Steuernagel Solar Simulator. Spectrally resolved photocurrent measurements were recorded by Lock-In technique, illuminating the device with ~ 0.1 mW/cm² monochromatized light from a Xe arc lamp and white light background illumination. Light intensities were measured by a calibrated Si photodiode.

Synthesis of the Poly(*n*-octylsulfinyl-*para*-phenylene ethylene) Precursor. A solution of 0.178 mol of *Na-ter*-butoxide and 0.181 mol of 1-octanethiol in 300 ml of methanol was added to a clear solution of 67.1 g Wessling salt in 200 ml of methanol. The mixture was stirred for another 30 min. The solvent was removed in vacuo. *n*-Octane was added and removed in vacuo (3 \times). The remaining oil was dissolved in CHCl₃ and washed with water and NaHCO₃ (1 M). The solution was finally dried on MgSO₄.

H₂O₂ was then added to a solution of the crude compound with TeO₂ in 300 mL of methanol/1,4-dioxane (5:1). After 5 h of stirring the reaction was stopped by adding 100 ml of a saturated NaCl solution. The mixture was then extracted with CHCl₃ and dried on MgSO₄. Yield: 43.4 g of crude monomer. The monomer α -chloro- α' -octylsulfinyl-*p*-xylene was further purified by crystallization from CHCl₃/hexane.

A 0.106 mol portion of *Na-ter*-butoxide in 240 ml of methanol was added all at once to a mechanically stirred solution of 0.082 mol of α -chloro- α' -octylsulfinyl-*p*-xylene in 570 ml of *s*-butanol. After 1 h of stirring, the mixture was poured into ice water, neutralized with HCl (1 M) and extracted with CHCl₃. The solvent was evaporated and the extract was redissolved in CHCl₃ and then precipitated in diethyl ether. The precipitate was collected and dried in vacuo. Yield: 14.7 g polymer; ¹H NMR (400 MHz, CDCl₃) δ 0.81, 1.17, 1.59, 1.96, 2.18, 2.26, 3.03, 3.62, 6.94; ¹³C NMR (400 MHz, CDCl₃) δ 14.0, 22.4, 22.5, 23.0, 28.7, 28.9, 29.0, 31.6, 36.3, 49.7, 65.2, 69.7, 128.4, 128.9, 129.4, 129.9, 131.5, 132.3, 138.2.

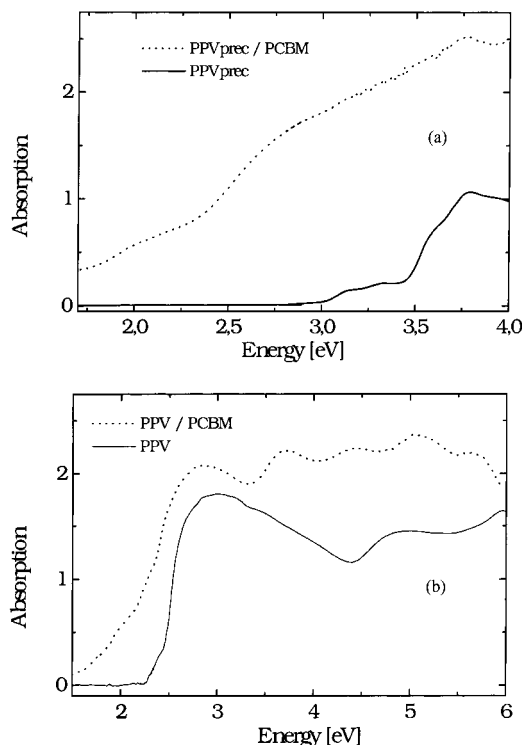


Figure 2. (a) UV-vis absorption spectra of the precursor polymer (—) and of the precursor polymer mixed with PCBM (···) on KBr substrates. (b) Absorption spectra of PPV (—) and the PPV/PCBM composite (···) after conversion.

Results and Discussion

UV-Vis Absorption. The complete conversion of the precursor polymer inside the composites with PCBM was evidenced by UV-vis and IR absorption. Figure 2, parts a and b, show the absorption spectrum of the *n*-octyl sulfinyl precursor with and without PCBM before and after the conversion step, respectively. The *n*-octyl sulfinyl precursor spectrum does not show absorption features in the visible region. A remarkable feature with a vibronic structure is detected between 3 and 4 eV with a maximum around 3.78 eV. Upon the addition of PCBM, the spectrum of the unconverted compound is dominated by the absorption features of PCBM. The onset of absorption is observed below 1.5 eV with the maximum at app. 3.74 eV. After the conversion, the color of the pristine polymer samples changed from transparent to an intense yellow as plotted in Figure 2b, proving the successful conversion process even for the blend. The build up of conjugation leads to a broad absorption band between 2.5 and 4.5 eV with the maximum peaking at 3 eV. A second, less intense transition is located at 5 eV. It is worthwhile to note that no long tail extending to lower energies due to scattering or reflectivity are observed in the fully converted samples. In the PPV samples investigated, no vibronic fine structure was observed.

During the conversion of the PPV/PCBM composites, the samples became slightly darker and less transparent. The surface of the converted samples was still homogeneous without visible defects or holes. The absorption spectrum of the PPV/PCBM composite is a linear superposition of the PPV and the PCBM absorption spectra. The build-up of conjugation is clearly observed by a peak arising at 2.78 eV, which was not observed in the precursor polymer/PCBM blend. The small shift compared to the absorption maximum of the pristine PPV sample is an artifact and comes from the background absorption of the PCBM. The fullerene peaks at 3.73 and at 4.43 eV became more

pronounced. Again, the second transition arising from the PPV is observed at 5.04 eV.

IR Absorption. Figure 3 presents the vibrational spectra of the precursor polymer with and without PCBM and after a 4 h conversion step at 180 °C under 10^{-2} mbar. The spectra have been scaled to the semicircle ring stretch mode at ~ 1516 cm^{-1} . Generally, the observed vibrational frequencies of this PPV agree with data published by other groups on PPV prepared from different precursor polymers.^{28–31} The region from 1700 to 2800 cm^{-1} , determined by the overtone and combination vibrational bands, is omitted in the Figures. No carbonyl contamination was observed in the pristine polymer samples as evidenced by the absence of C=O stretching vibration at about 1690 cm^{-1} .

The progress of the thermal conversion is monitored by the relative decrease of the bands at 1045, 1464, 2842, 2924, and 2953 cm^{-1} , and the relative increase of the bands at 557, 837, 962, and 3024 cm^{-1} observed for the samples with and without PCBM. The vanishing bands, usually associated with the CH_3 respectively CH_2 vibrations,^{28,30} are also observed in the precursor polymer with higher intensity compared to the 1516 cm^{-1} vibration. Longer conversion times and/or higher vacuum completely quench the bands at 1045 and 1464 cm^{-1} . Figure 3e shows the IR absorption for a sample with 10 wt % PCBM which was converted at a vacuum better than 10^{-4} mbar. The lower fullerene content allows us to observe the polymer bands more clearly and rather complete conversion is manifested. The bands seen at 964 and 3022 cm^{-1} are associated with the vibrations of the unsaturated vinylene groups and gain intensity during the conversion. No substantial change in the vibrations of the *para*-phenylene unit appears during the conversion reaction. The strongest ring stretching vibration shifts from 1512 to 1516 cm^{-1} . This shift is indicative of an increase of the electron donating character of the substituents of the phenylene ring.^{30,32} The infrared spectra of the polymer mixed with PCBM are complicated due to the numerous absorption bands of the methanofullerene, which are reported elsewhere.²⁶ However, the same peaks as for the pristine polymer can be identified and successful conversion of the precursor polymer to the PPV can be monitored. The PPV/PCBM composite did not show additional bands as compared to a PPV and a PCBM spectrum. No formation of new chemical bonds except the one due to the conversion of the precursor was observed.

These results from UV–vis and IR absorption show that the conversion of the precursor polymer to PPV is not hindered by the presence of the methanofullerene PCBM. No hints were observed that the elimination of the precursor-PPV/PCBM composites leads to chemical reactions between the polymer and the methanofullerene or other side reactions.

Luminescence Quenching. The photoluminescence of the PPV sample at room temperature, pumped at 3.1 eV, is shown in Figure 4a, together with the room-temperature photoluminescence of the PPV/PCBM composite. The rather broad photoluminescence starts below 1.8 eV and shows the maximum at 2.25 eV with a well-pronounced shoulder at 2.07 eV. Additionally, a small shoulder is observed at ~ 2.41 eV. The excitation profile of the two emission features at 2.07 and 2.25 eV have identical shapes. The maximum of the emission spectrum is red shifted by 0.5 eV compared to the maximum of the absorption spectrum. The intense photoluminescence of the PPV is almost quenched completely for the PPV/PCBM composite. The intensity is reduced in the composite by at least 3 orders of magnitude. The shape of the PPV luminescence and the weights of the vibronic progression have changed consider-

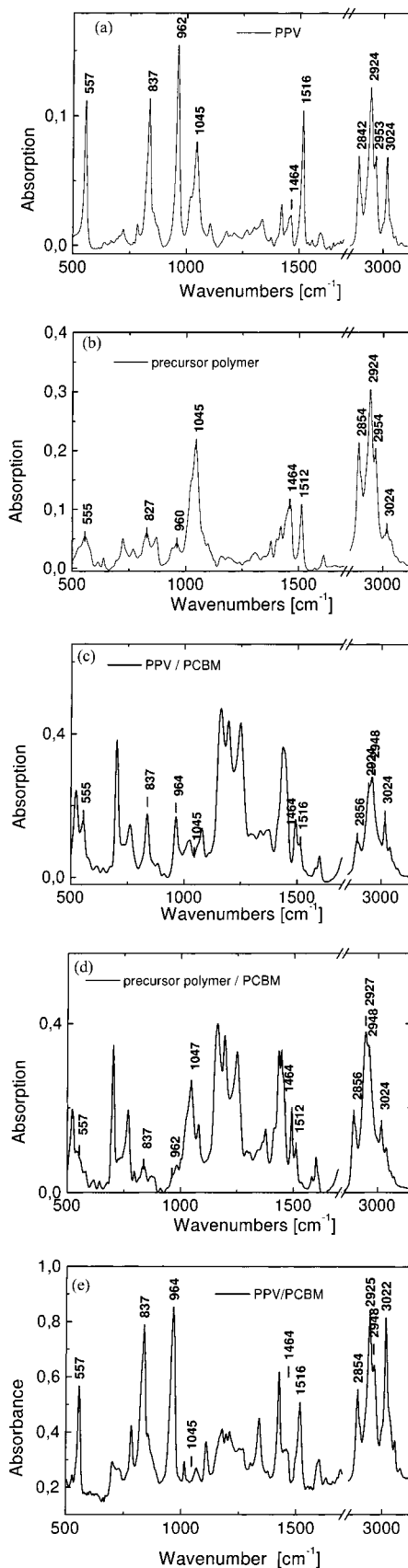


Figure 3. Infrared absorption spectra of (a) the precursor polymer, (b) of converted PPV, (c) of a precursor polymer/PCBM composite and (d) of the PPV/PCBM composite. (e) shows the IR spectrum of a 10% PCBM composite after conversion under high vacuum.

ably at low temperatures (Figure 4b) as compared to the room-temperature luminescence. At low temperatures, the $\text{S}_1 \rightarrow \text{S}_0$

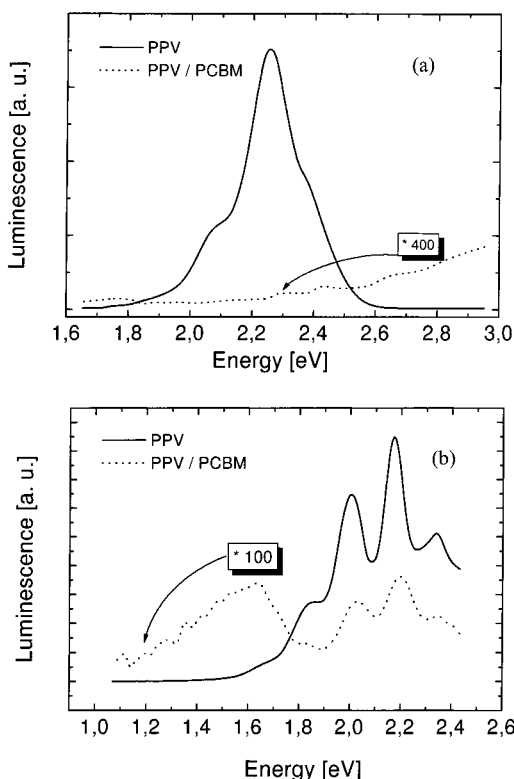


Figure 4. (a) Room-temperature luminescence of PPV (—) and PPV/PCBM (···, times 400) on KBr pellets. Luminescence was measured in 90° geometry excited at 400 nm. (b) Luminescence of PPV (—) and PPV/PCBM (···, ×100) on glass substrates at 100 K. Luminescence was measured in reflection geometry. Excitation was provided by Ar⁺ laser beam with 2.54 eV, chopped at 132 Hz.

(0 → 0) transition can be identified at 2.34 eV. The maximum of luminescence is found for the S1 → S0(0 → 1) transition at 2.17 eV. The red shift of the S1 → S0(0 → 1) when going from 100 K to room temperature is about 80 meV. At 100 K, the separation between the S1 → S0(0 → 0) transition and the S1 → S0(0 → 1) transition is found to be 170 meV. Even for the PPV/PCBM sample, the characteristic PPV luminescence is observed with good resolved vibronic progression, although quenched by at least 300 times. However, the whole spectrum is blue-shifted by ~25 meV. This blueshift was also observed in blends of alkoxy PPVs with fullerenes.³³ In the PPV/PCBM composite, a weak emission is observed at 1.63 eV, which cannot originate from PPV as it is absent in the pristine polymer sample. Uncharged PCBM has a weak emission in this spectral region, most probably due to the singlet emission of the fullerene.³³

These luminescence studies indicate a rapid photoinduced charge transfer in the bulk of PPV/PCBM composites as observed for other alkoxy PPV/fullerene blends.²

PIA FTIR. The PIA-IR spectrum of the PPV drop cast film on KBr is shown in Figure 5a together with the spectrum of a PPV/PCBM composite. Figure 5b zooms in the low energy part of the PIA-IR spectrum of the PPV/PCBM sample. The PPV/PCBM composite reveals a subgap electronic absorption band at 3800 cm⁻¹, which is enhanced by a factor of 4 compared to pristine PPV sample. In addition, strong IRAV bands are seen at 1112, 1276, 1313, 1413, and 1479 cm⁻¹ for the PPV/PCBM sample. Again, these IRAV bands are much weaker in the pristine PPV sample. The IRAV bands observed for this PPV from the *n*-octyl sulfinyl precursor agree with data published by other groups on PPV prepared from different precursor polymers. The occurrence of enhanced IRAV bands is widely

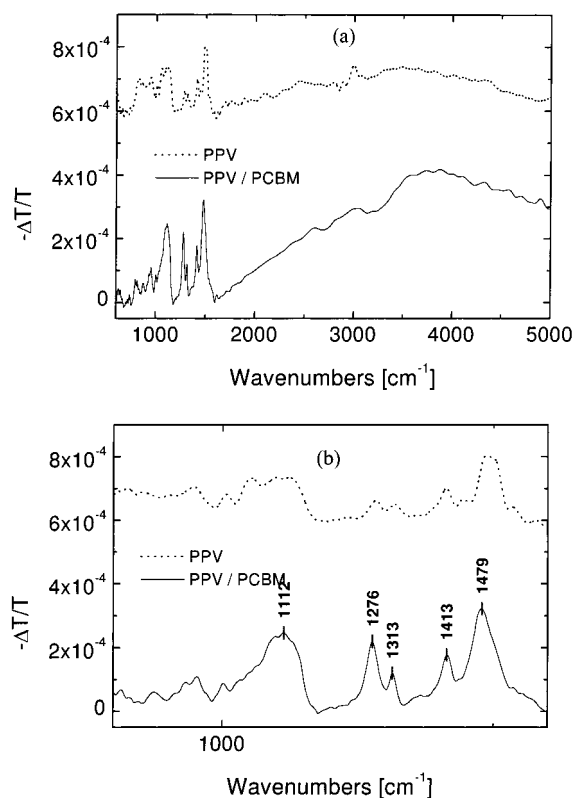


Figure 5. (a) PIA IR spectrum of PPV (···), shifted on the y-axis, and of PPV/PCBM (—) from drop cast films on KBr at 100 K. Excitation was provided by an Ar⁺ laser beam at 2.54 eV with 20 mW. (b) Zoom to the IRAV bands.

considered as evidence of an enhanced photogeneration of charges.³⁴ This effect indicates further a photoinduced charge transfer from PPV to PCBM.

UV–vis PIA. Figure 6 shows the photoinduced absorption spectrum (PIA) of (a) pristine PPV and of (b) a PPV/PCBM composite together with the phase angle at 100 K. The luminescence background was subtracted from the signal shown. For pristine PPV, the weak signal observed is a rather broad, unspecific peak. The signal arises at 1.3 eV and remains almost at a constant strength until 2 eV. A small shoulder can be seen at 1.48 eV. The photoinduced absorption was measured for different frequencies from 13 Hz up to 300 Hz, yielding similar results. The lifetime of the signal can therefore be estimated to be smaller than 1 ms.

The addition of PCBM changes the size of the signal by nearly 2 orders of magnitude. Again, a broad signal from 1.3 to 2.0 eV with a shoulder at 1.46 eV is observed.

In analogy to PIA studies on alkoxy-PPV/PCBM,³³ alkoxy-PPV/tetracyano-anthraquino-dimethane (TCAQ) derivative³⁵ composites and previous studies on pristine PPV from different precursor polymers^{36,37} the photoinduced absorption features between 1.3 and 2.0 eV are assigned to the high energy absorption of photogenerated polarons on PPV. The quasi-steady state density of the PPV polarons with a lifetime less than 1 ms is enhanced by nearly 2 orders of magnitude upon the addition of PCBM, evidencing the rapid photoinduced charge transfer between the polymer and the fullerene. For all the measurements, we were unable to detect any sign of a triplet–triplet absorption. It was also reported earlier that photoinduced triplet absorption in PPV is observed only for specific sample preparation and at low measurement temperatures (below 80 K).^{36,37}

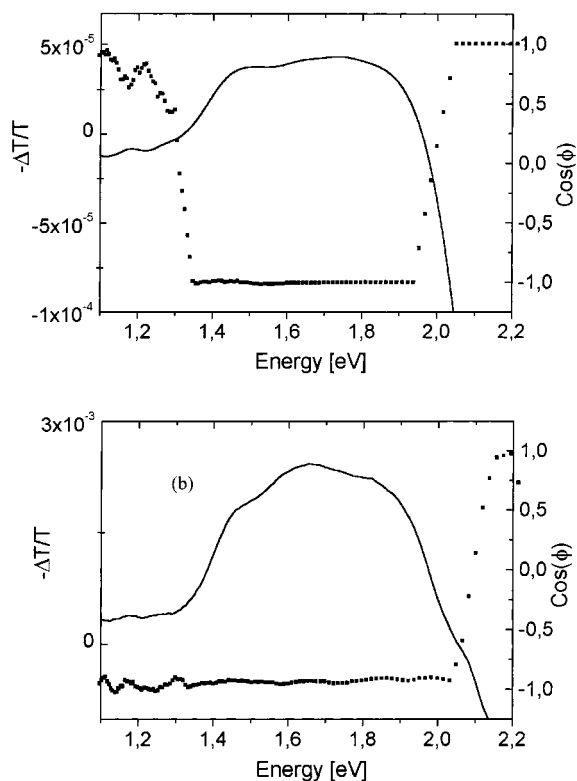


Figure 6. (a) PIA spectrum (---) and the phase angle ϕ (\blacksquare) of (a) a PPV drop cast and (b) a PPV/PCBM drop cast film on glass substrates at 100 K. Excitation was provided by an Ar^+ laser beam at 2.54 eV, chopped at 132 Hz.

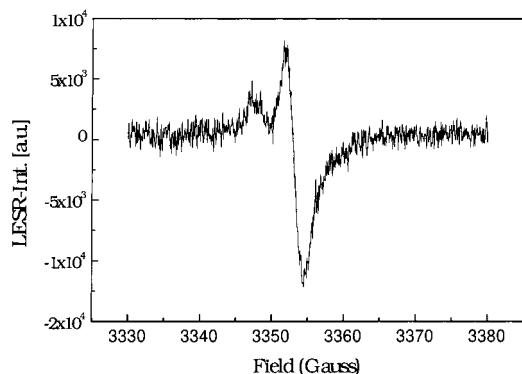


Figure 7. LESR spectrum of a free-standing film of a PPV/PCBM composite in a 2-methyl THF glass at 100 K. Spectra were taken at 10 mW microwave power under Ar^+ laser illumination of ~ 100 mW.

Comparing the enhancement in the signal magnitude of ΔT upon addition of PCBM, a factor of ~ 40 is observed for the UV-vis PIA measurement compared to a factor of ~ 5 for the PIA FTIR measurement (see Figures 5 compared to Figures 6). This difference is explained by the different sensitivity of the two measurement methods to long living charges. We consider the lock-in measurements (Figures 6) to give a more reliable factor for the enhancement of photoinduced charge carriers in composites of PPV with PCBM since this technique is not sensitive for long living, probably trapped charge carriers (i.e., charge carriers with a lifetime τ larger than the inverse chopping frequency $1/\omega$).

LESR. The LESR spectrum plotted in Figure 7 shows two features, one at $g \approx 2.0000$ and another one with $g \approx 2.0025$. No dark ESR signals were observed. The assignment of the $g \approx 2.0000$ feature to the PCBM^- radical anion is in agreement with recent studies on MDMO-PPV/PCBM composites.²⁷ The

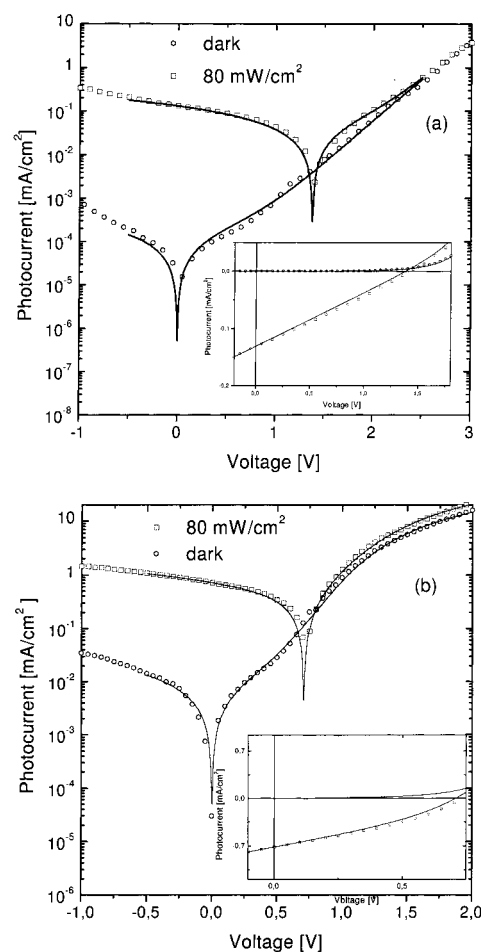


Figure 8. Logarithmic and linear (inset) plot of the I/V curves for (a) a PPV diode and (b) a PPV/PCBM diode under white light illumination with 80 mW/cm^2 (\square) and in the dark (\circ). The lines are fits from a single diode model with the parameters given in Table 1.

$g \approx 2.0025$ feature is assigned to the PPV^+ polaron and shows excellent correlation with the positive polaron on substituted alkoxy PPVs.²⁷

Photovoltaic Devices. Photovoltaic devices were produced from PPV/PCBM (1:3 wt ratio) solutions as described in the Experimental Section. ITO/PEDOT glass substrates were used as cathodes, whereas for the anode, a thin layer of LiF was applied before thermally evaporating Al with a thickness of 80 nm. This technique has been shown to enhance the interface between the active layer and the cathode in organic light-emitting diodes.^{38,39} Figure 8a shows the I/V curve of a pristine PPV diode, whereas Figure 8b shows the I/V characteristics of a PPV/PCBM diode in the dark and under illumination with 80 mW/cm^2 white light from a solar simulator. The symbols in the plots represent the measurement data while the thick lines are fits to a one diode model, according to

$$I(V) = I_0 (\exp(q(V - IR_s)/nkT) - 1) + (V - IR_s)/R_p + I_{sc} \quad (1)$$

where I_0 , R_s , R_p , n , and q/kT are the saturation current density, the serial and parallel resistivity, the diode ideality factor and the temperature potential (25 mV at room temperature), respectively. For all diodes, good fits could be generated with the one diode model. The diode parameters in the dark and under illumination are given in Table 1a and Table 1b, whereas the solar cell parameters are given in Table 1c. We want to emphasize that the analysis of the diode parameters does not rely on a specific diode model (like, for instance, a Schottky

TABLE 1: (A) Diode Parameters Derived from a Single Diode Model for (a) PPV and PPV/PCBM Diodes in the Dark, (B) PPV, PPV/PCBM and MDMO-PPV/PCBM Diodes Illuminated with 80 mW/cm² of White Light, and (C) Photovoltaic Parameters of PPV, PPV/PCBM, and MDMO-PPV/PCBM Diodes under the Same Illumination conditions

A	I_0 [mA/cm ²]	R_s [Ω cm ²]	R_p [Ω cm ²]	n	
PPV	6.962×10^{-6}	38.89	$3.62 \times 10^{+6}$	8.8	
PPV/PCBM	4.51×10^{-4}	43.79	$3.88 \times 10^{+7}$	5.2	
B	I_0 [mA/cm ²]	R_s [Ω cm ²]	R_p [Ω cm ²]	n	
PPV	4.195×10^{-6}	18.89	$8.58 \times 10^{+3}$	8.34	
PPV/PCBM	3.643×10^{-3}	27.29	$1.45 \times 10^{+3}$	6.2	
MDMO-PPV/ PCBM	2.394×10^{-8}	3.55	$0.978 \times 10^{+3}$	1.8	
C	I_{sc} [mA/cm ²]	V_{oc} [mV]	FF	IPCE [%]	η [%]
PPV	-0.13	1400	0.25	2.5	0.056
PPV/PCBM	-0.72	720	0.37	13	0.24
MDMO-PPV/ PCBM	-2.324	820	0.5	25	1.2

model or p-n junction model) but only allows to discuss general transport phenomena.

The serial as well as the parallel resistance of the PPV diode is comparable to the PPV/PCBM diode. Some photoconductivity under forward bias is observed for both diodes. The ideality factors n for both diodes are too large ($5 < n < 9$) to be explained by the classical p-n diode model with defect assisted recombination and are frequently interpreted as an indication for a tunneling component contributing to the diode current⁴⁰ or as an indication for inhomogeneous current paths within the bulk.⁴¹

Upon addition of PCBM, a nearly 5-fold increase in the short circuit current is observed. This factor is rather small compared to other alkoxy substituted PPV/C₆₀ diodes, where current sensitization of up to two orders in magnitude were reported upon fullerene addition.⁴² Obviously, photocarrier generation in these thin film PPV diodes is quite efficient compared to alkoxy substituted PPV diodes. The observation of an V_{oc} of 1400 mV for the pristine PPV diode is in agreement with the MIM⁴³ model suggested recently for conjugated polymer diodes with low defect densities. The lowering of the open circuit voltage upon addition of PCBM ($V_{oc} \sim 720$ mV) can be explained with the lowering of the quasi-Fermi level due to the energy loss of the electron during the electron transfer from the PPV to the PCBM.^{44,45} The overall white light efficiency of the devices is calculated with 0.056% for the pristine PPV diodes and with 0.24% for the PPV/PCBM diodes which are among the highest values reported in the literature for PPV based diodes.⁴⁶

Figure 9 compares the spectrally resolved photocurrent of a PPV (a), a PPV/PCBM (b), and a MDMO-PPV/PCBM (c) device together with the absorption spectra of thin films, spin cast on glass with comparable thickness. The incident photon to converted electron efficiency (IPCE) was calculated as reported earlier,⁴⁷ and the peak values are listed in Table 1c. Generally, the relationship between absorption and spectrally resolved photocurrent may be classified into two categories: A good correlation between the spectra, such that the maximal photocurrent is found for excitation at the peak of the absorption spectrum, is said to be symbatic. If the maximum of the

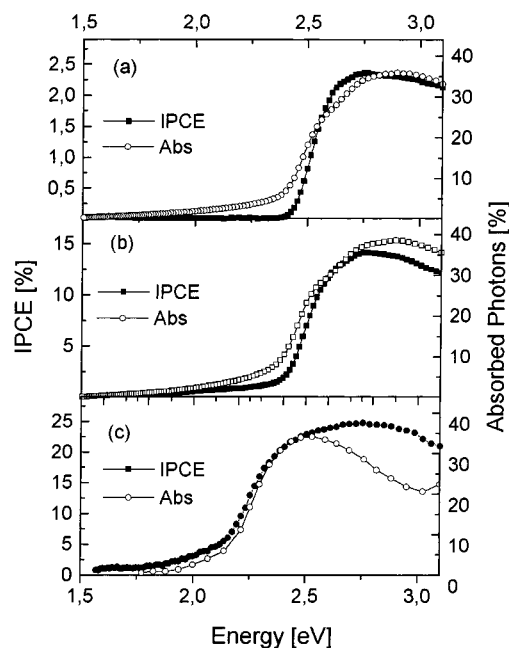


Figure 9. Incident photon to converted electron (IPCE) efficiency (■) for photodiodes comprising an active layer of (a) PPV, (b) PPV/PCBM and (c) MDMO-PPV/PCBM. On the right-hand axis, the fraction of photons absorbed in films with comparable thickness spin cast on glass (○) are plotted.

photocurrent occurs for photon energies where the optical absorption is very weak (filter effect), the correlation is said to be antibatic.

Antibatic behavior was reported for ITO/PPV/Al photovoltaic devices, independent of the illumination direction as long as the light intensities were low and the PPV layer thick enough.⁴⁸ Generally, the same spectral photocurrent features as for PPV diodes were recently observed in the case of pristine alkoxy-PPV diodes.⁴⁹ For the PPV diodes investigated in this study, rather good correlation of the photocurrent with the absorption is observed for energies higher than 2.5 eV, whereas the low energy tail of the absorption does not contribute to the photocurrent (Figure 9a). From the onset of the photocurrent, we estimate the band gap of PPV with ~ 2.4 eV, which is in good agreement with literature. The more pronounced symbatic behavior, observed qualitatively for the PPV/PCBM diodes, is a strong indication for direct charge generation within the whole absorptive region as well as for rather balanced hole and electron mobilities. Further, for the PPV/PCBM diodes (Figure 9b), photocurrent generation in the spectral region between 1.8 and 2.4 eV is observed and assigned to a hole transfer from the photoexcited PCBM to the PPV. The PPV/PCBM photocurrent spectrum qualitatively shows similar symbatic behavior as the reference diode produced from MDMO-PPV/PCBM and plotted in Figure 9c. Quantitatively, the peak value of the IPCE for the photodiode produced from alkoxy PPV/PCBM is nearly twice as large as for the PPV/PCBM diode.

Figure 10 compares the I/V characteristics of an illuminated PPV/PCBM diode with the characteristics of the MDMO-PPV/PCBM diode. Again, the symbols represent the measurement data while the lines are fits from a one diode model. The diode and the solar cell parameters are given in Table 1, parts B and C.

For both diodes a comparable parallel resistance is observed, indicating that shunts play a negligible role for these devices. A clear difference is observed for the serial resistance. For the MDMO-PPV/PCBM device, R_s is nearly 1 order of magnitude

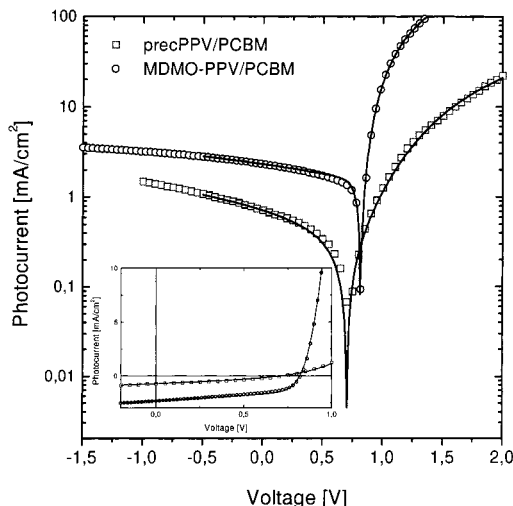


Figure 10. Logarithmic and linear (inset) plot of the I/V curves for a PPV/PCBM diode (□) compared to a MDMO-PPV/PCBM (○) diode under white light illumination with 80 mW/cm². The lines are fits from a one diode model with the parameters given in Table 1.

lower than for the PPV/PCBM device, whereas comparable values are observed for PPV diodes with and without PCBM. This indicates that the PPV is responsible for the larger serial resistance. This large serial resistance is also mirrored in the lower filling factor of the PPV/PCBM diode. A significant difference is observed in the ideality factor as well as in the saturation current. For the MDMO-PPV/PCBM diode, the ideality factor is calculated $n \approx 1.8$ compared to $n \approx 6.2$ for the PPV/PCBM diode. At least one additional recombination process yielding a diode ideality factor with $n > 2$ must be taken into account to explain the large n calculated for the PPV/PCBM diodes. Furthermore, the saturation current of the MDMO-PPV/PCBM diode is nearly 5 orders of magnitude smaller than for the PPV/PCBM diode. Independently of the microscopic model for the diode (thermionic emission at a metal-semiconductor interface or diffusion at a p-n junction), large saturation currents in solar cells, which reduce the fill factor as well as the open circuit voltage, indicate efficiency diminishing processes. Following the analysis of Pope⁵⁰ by solving the one-dimensional diffusion equation under the assumption that there is only one type of carrier, the following formula was derived for the saturation current

$$I_0 = q n_0^d v_r \quad (2)$$

where n_0^d is the carrier density at the polymer/metal interface, and v_r is the recombination velocity which is proportional to the number of recombination sites. Therefore, a possible mechanism explaining the larger saturation current in PPV compared to MDMO-PPV is the recombination between injected and intrinsic carriers of different signs. From the peak values of the IPCE (25% compared to 13%), the upper limit of photogenerated carriers lost due to recombination can be estimated by a factor of 2. Comparison of the short circuit currents under white light illumination (2.32 mA/cm² compared to 0.72 mA/cm²) reflects both, the enhanced recombination but also the blue-shift of the PPV absorption spectrum compared to MDMO-PPV.

Finally, the nearly 5-fold lower power efficiency of the PPV diodes compared to the alkoxy-PPV diodes (0.25% compared to 1.2%) is caused by the interplay of diode properties (increased serial resistance, larger saturation current), enhanced recombination and a larger mismatch to the solar spectrum.

Conclusion

Photoinduced charge transfer in composites of PPV prepared from a novel precursor polymer blended with the methanofullerene PCBM was studied. The production and processing of such composites was enabled due to the solubility of this novel precursor polymer in common organic solvents. The conversion of the precursor polymer to PPV was not influenced by the presence of PCBM. All spectroscopic investigations show that these PPV/PCBM composites exhibit an efficient photoinduced charge transfer within the bulk similar to composites of soluble alkoxy-PPVs and fullerenes. Photovoltaic devices with interesting quantum efficiencies were prepared, proving the application potential of this precursor polymer. Comparison of the diode and the photovoltaic properties of the PPV/PCBM diodes with the performance of alkoxy-PPV/PCBM diodes allows the conclusion that recombination plays a more important role in the PPV diodes than in alkoxy PPV diodes. This finding is further supported by the observation of long living carriers by IR-PIA spectroscopy. Additional interest in this polymer stems from the fact that it has a rather low glass temperature and can be oriented by rheological methods. Investigations are in progress to prepare and characterize mechanically stretch-oriented films and devices.

Acknowledgment. This work was performed within the Christian Doppler Society dedicated laboratory on Plastic Solar Cells funded by the Austrian Ministry of Economic Affairs and Quantum Solar Energy Linz Ges. m.b.H. The work was further supported by the "Fonds zur Förderung der wissenschaftlichen Forschung" of Austria (Project No. P-12680-CHE), the Magistrat Linz and The Netherlands Organization for Energy & Environment (NOVEM). Additional support has been obtained from the National Science Foundation - Flanders.

References and Notes

- (1) Kanicki, J. In *Handbook of Conducting Polymers*; Skotheim, T. A., Ed.; Marcel Dekker: New York, Vol. 1, 1985.
- (2) Sariciftci, N. S.; Smilowitz, L.; Heeger, A. J.; Wudl, F. *Science* **1992**, *258*, 1474.
- (3) Sariciftci, N. S.; Baun, D.; Zhang, C.; Srdanov, V. I.; Heeger, A. J.; Stucky, G.; Wudl, F. *Appl. Phys. Lett.* **1993**, *62*, 585.
- (4) Yu, G.; Gao, J.; Hummelen, J. C.; Wudl, F.; Heeger, A. J. *Science* **1995**, *270*, 1789.
- (5) Sariciftci, N. S.; Heeger, A. J. In *Handbook of Organic Conductive Molecules and Polymers*; Nalwa, H. S., Ed.; John Wiley & Sons: New York, Vol. 1, 1997.
- (6) Horovitz, G. *Adv. Mater* **1989**, *2*, 287.
- (7) Glenis, S.; Tourillon, G.; Garnier, F. *Thin Solid Films* **1986**, *139*, 221.
- (8) Marks, R. N.; Halls, J. J. M.; Bradley, D. D.; Friend, R. H.; Holmes, A. B. *J. Phys. Condens. Matter* **1994**, *6*, 1379.
- (9) Burroughes, J. H.; Bradley, D. D.; Brown, C. A. R.; Marks, R. N.; Mackay, K.; Friend, R. H.; Burn, P. L.; Holmes, A. B. *Nature* **1990**, *347*, 539.
- (10) Braun, D.; Heeger, A. J. *Appl. Phys. Lett.* **1991**, *58*, 1982.
- (11) Braun, D.; Heeger, A. J.; Kroemer, H. *J. Electron. Mater.* **1991**, *20*, 945.
- (12) Greenham, N. C.; Moratti, S. C.; Bradley, D. D. C.; Friend, R. H.; Holmes, A. B. *Nature* **1993**, *365*, 628.
- (13) Yu, G.; Zhang, C.; Heeger, A. J. *Appl. Phys. Lett.* **1994**, *64*, 1540.
- (14) Smilowitz, L.; Sariciftci, N. S.; Wu, R.; Gettinger, C.; Heeger, A. J.; Wudl, F. *Phys. Rev. B* **1993**, *47*, 13 835.
- (15) Kraabel, B.; Hummelen, J. C.; Vacar, D.; Moses, D.; Sariciftci, N. S.; Heeger, A. J.; Wudl, F. *J. Chem. Phys.* **1996**, *104*, 4267.
- (16) Sariciftci, N. S.; Heeger, A. J. *Int. J. Mod. Phys. B* **1994**, *8*, 237.
- (17) Sariciftci, N. S. *Prog. Quant. Electr.* **1995**, *19*, 131.
- (18) Wei, X.; Vardeny, Z. V.; Sariciftci, N. S.; Heeger, A. J. *Phys. Rev. B* **1996**, *53*, 2187.
- (19) Morita, S.; Zakhidov, A. A.; Yoshino, K. *Solid State Commun.* **1992**, *82*, 249.
- (20) Yoshino, K.; Yin, X. H.; Morita, S.; Kawai, T.; Zakhidov, A. A. *Solid State Commun.* **1993**, *85*, 85.

- (21) Morita, S.; Zakhidov, A. A.; Yoshino, K. *Jpn. J. Appl. Phys.* **1993**, *32*, L873.
- (22) Yoshino, K.; Akashi, T.; Yoshimoto, K.; Morita, S.; Sugimoto, R.; Zakhidov, A. A. *Solid State Commun.* **1994**, *90*, 41.
- (23) Feldrapp, K.; Brütting, W.; Schwoerer, M.; Brettreich, M.; Hirsch, A. *Synthetic Metals* **1999**, *101*, 156.
- (24) (a) Issaris, A.; Vanderzande, D.; Gelan, J. *Polymer* **1997**, *38*, 2571. (b) Louwet, F.; Vanderzande, D.; Gelan, J.; Mullens, J. *Macromol.* **1995**, *28*, 1330. (c) van Breemen, A. J. A. J.; Issaris, A. C. J.; de Kok, M. M.; Van Der Borght, M. J. A. N.; Adriaenssens, P. J.; Gelan, J. M. J. V.; Vanderzande, D. J. *Macromolecules* **1999**, *32* (18), 5728.
- (25) de Kok, M. M.; Nguyen, T. P.; Molinie, P.; van Breemen, A. J. J. M.; Vanderzande, D. J.; Gelan, J. M. *Synth. Met.* **1999**, *102*, 949.
- (26) Hummelen, J. C.; Knight, B. W.; Lepec, F.; Wudl, F.; Yao, J.; Wilkins, C. L. *J. Org. Chem.* **1995**, *60*, 532.
- (27) Dyakonov, V.; Zorinians, G.; Scharber, M. C.; Brabec, C. J.; Janssen, R. A. J.; Hummelen, J. C.; Sariciftci, N. S. *Phys. Rev. B* **1999**, *59*, 8019.
- (28) Voss, K. F.; Foster, C. M.; Smilowitz, L.; Mihailovic, D.; Askari, S.; Srdanov, G.; Ni, Z.; Shi, S.; Heeger, A. J.; Wudl, F. *Phys. Rev. B* **1991**, *42*, 5109.
- (29) Bradley, D. D. C. *J. Phys. D* **1987**, *20*, 1389.
- (30) Bradley, D. D. C.; Friend, R. H.; Lindenberger, H.; Roth, S. *Polymer* **1986**, *27*, 1709.
- (31) Sakamoto, A.; Furukawa, Y.; Tasumi, M. *J. Phys. Chem.* **1992**, *96*, 1490.
- (32) Katritzky, A. R. *Quart. Rev.* **1959**, *13*, 353.
- (33) Brabec, C. J.; Dyakonov, V.; Sariciftci, N. S.; Graupner, W.; Leising, G.; Hummelen, J. C. *J. Chem. Phys.* **1998**, *109*, 1185.
- (34) Vardeny, Z. V.; Ehrenfreund, E.; Brafman, O.; Heeger, A. J.; Wudl, F. *Synth. Met.* **1987**, *18*, 183. Zerbi, G.; Gussoni, M.; Castiglioni, C. In *Conjugated Polymers*; Brédas, J. L., Silbey, R., Eds.; Kluwer Academic Publishers: New York, 1991, 435–507. Zerbi, G.; Castiglioni, C.; Del Zoppo, M. In *Electronic Materials: The Oligomer Approach*; Müllen, K., Wegner, G., Eds.; Wiley-VCH: New York, 1998, 345–402.
- (35) Zerza, G.; Scharber, M.; Brabec, C. J.; Sariciftci, N. S.; Segura, J.; Martin, N. *J. Phys. Chem. A* **2000**, *104*, 8315.
- (36) Wei, X.; Hess, C. B.; Vardeny, Z. V.; Wudl, F. *Phys. Rev. Lett.* **1992**, *68*, 666.
- (37) Colaneri, N. F.; Bradley, D. D.; Friend, C. R. H.; Burn, P. L.; Holmes, A. B.; Spangler, C. W. *Phys. Rev. B* **1990**, *42*, 11670.
- (38) Hung, L. S.; Tang, C. W.; Mason, M. G. *Appl. Phys. Lett.* **1997**, *70*, 152.
- (39) Jabbour, G. E.; Kawabe, Y.; Shaheen, S. E.; Wang, J. F.; Morrell, M. M.; Kippelen, B.; Peyghambarian, N. *Appl. Phys. Lett.* **1997**, *71*, 1762–1764.
- (40) Sze, S. M. *Physics of Semiconductor Devices, 2nd ed.*; John Wiley & Sons: New York, 1981.
- (41) Meissner, D., private communication.
- (42) Gao, J.; Hide, F.; Wang, H. *Synth. Met* **1997**, *84*, 979.
- (43) Parker, I. D. *J. Appl. Phys.* **1994**, *75*, 1656.
- (44) Campbell, L. H.; Hagler, T. W.; Smith, D. L.; Ferraris, J. P. *Phys. Rev. Lett.* **1996**, *76*, 1900.
- (45) Heller, C. M.; Campbell, I. H.; Smith, D. L.; Barashkov, N. N.; Ferraris, J. P. *J. Appl. Phys.* **1997**, *81*, 3217.
- (46) Antoniadis, H.; Hsieh, B. R.; Abkowitz, M. A.; Stolka, M.; Jenekhe, S. A. *Polym. Prepr.* **1993**, *34*, 490. Antoniadis, H.; Hsieh, B. R.; Abkowitz, M. A.; Jenekhe, S. A.; Stolka, M. *Synth. Met.* **1994**, *62*, 265.
- (47) Brabec, C. J.; Padinger, F.; Hummelen, J. C.; Sariciftci, N. S. *J. Appl. Phys.* **1999**, *85*, 6866.
- (48) Riess, W.; Karg, S.; Dyakonov, V.; Meier, M.; Schwoerer, M. *J. Lumin.* **1994**, *60&61*, 906.
- (49) Harrison, M. G.; Grüner, J.; Spencer, G. C. W. *Phys. Rev. B* **1996**, *55*, 7831.
- (50) Pope, M.; Swenberg, C. E. *Electronic Processes in Organic Crystals and Polymers*; Chapter II/I; Oxford University Press: Oxford, 1999.